Atmospheric Environment 131 (2016) 17–28

Contents lists available at ScienceDirect

Atmospheric Environment

journal homepage: www.elsevier.com/locate/atmosenv

Mid-twentieth century increases in anthropogenic Pb, Cd and Cu in central Asia set in hemispheric perspective using Tien Shan ice core

B. Grigholm [a, *], P.A. Mayewski [a], V. Aizen [b], K. Kreutz [a], C.P. Wake [c], E. Aizen [b], S. Kang [d, e], K.A. Maasch [a], M.J. Handley [a], S.B. Sneed [a]

[a] Climate Change Institute and School of Earth and Climate Sciences, University of Maine, 133 Sawyer Environmental Research Center, Orono, ME 04469, USA
[b] Department of Geography, University of Idaho, Moscow, ID 83844-3025, USA
[c] Earth Systems Research Center, Institute for the Study of Earth, Oceans and Space, University of New Hampshire, Durham, NH 03824-3525, USA
[d] State Key Laboratory of Cryospheric Sciences, Cold and Arid Regions Environmental and Engineering Research Institute, Chinese Academy of Sciences, Lanzhou 730000, China
[e] CAS Center for Excellence in Tibetan Plateau Earth Sciences, Chinese Academy of Sciences, Beijing, China

HIGHLIGHTS

- Major/trace element records (1908–1995) were retrieved from central Asian ice core.
- Pb, Cd and Cu reveal anthropogenic contributions beginning in the 1950s.
- Pb, Cd and Cu reflect anthropogenic emissions from the Soviet Union and China.
- Anthropogenic sources include non-ferrous metals, coal and phosphate fertilizers.

ARTICLE INFO

Article history:
Received 23 September 2015
Received in revised form
14 January 2016
Accepted 18 January 2016
Available online 22 January 2016

Keywords:
Ice core
Element
Pollution
Central Asia
Tien Shan

ABSTRACT

High-resolution major and trace element (Al, As, Ca, Cd, Co, Cr, Cu, Fe, Li, Mn, Na, Pb, S, Ti, and V) ice core records from Inilchek glacier (5120 m above sea level) on the northwestern margin of the Tibetan Plateau provide the first multi-decadal ice core record spanning the period 1908–1995 AD in central Tien Shan. The trace element records reveal pronounced temporal baseline trends and concentration maxima characteristic of post-1950 anthropogenic emissions. Examination of Pb, Cd and Cu concentrations, along with non-crustal calculation estimates (i.e. excess (ex) and enrichment factor (EF)), reveal that discernable anthropogenic inputs began during the 1950s and rapidly increased to the late-1970s and early 1980s, by factors up to of 5, 6 and 3, respectively, relative to a 1910–1950 means. Pb, Cd and Cu concentrations between the 1950s-1980s are reflective of large-scale Soviet industrial and agricultural development, including the growth of production and/or consumption of the non-ferrous metals, coal and phosphate fertilizers. NOAA HYSPLIT back-trajectory frequency analysis suggests pollutant sources originating primarily from southern Kazakhstan (e.g. Shymkent and Balkhash) and the Fergana Valley (located in Kazakhstan, Uzbekistan and Kyrgyzstan). Inilchek ice core Pb, Cd and Cu reveals declines during the 1980s concurrent with Soviet economic declines, however, due to the rapid industrial and agricultural growth of western China, Pb, Cd and Cu trends increase during the 1990s reflecting a transition from primarily central Asian sources to emission sources from western China (e.g. Xinjiang Province).

1. Introduction

Rapid twentieth century growth of industry and agriculture has led to large-scale increases in heavy metal concentrations in air, water and soil, threatening natural ecosystems and human health (Pacyna and Pacyna, 2001; Järup, 2003). Major anthropogenic

* Corresponding author.
E-mail addresses: bjorn.grigholm@maine.edu (B. Grigholm), paul.mayewski@maine.edu (P.A. Mayewski), aizen@uidaho.edu (V. Aizen), karl.kreutz@maine.edu (K. Kreutz), cameron.wake@unh.edu (C.P. Wake), eaizen@uidaho.edu (E. Aizen), shichang.kang@lzb.ac.cn (S. Kang), kirk.maasch@maine.edu (K.A. Maasch), handley@maine.edu (M.J. Handley), Sharon.sneed@maine.edu (S.B. Sneed).

http://dx.doi.org/10.1016/j.atmosenv.2016.01.030

sources include non-ferrous metal production, fossil fuel combustion (e.g. leaded gasoline, oil and coal), fertilizers and waste incineration. Human exposure to these heavy metals (e.g. Pb and Cd) can result in both acute and chronic ailments including detrimental impacts to the development of the nervous system and severe respiratory, kidney and bone disorders (Järup, 2003). The spatial impacts of heavy metal emissions can vary from local to global, as pollutants can be deposited near the emission source and transported long-distances (Knutson and Tu, 1996; Pacyna and Pacyna, 2001). In recent decades research via various monitoring programs and emission inventories have been conducted to assess the impacts of heavy metals (e.g. Nriagu and Pacyna, 1988; Pacyna and Pacyna, 2001). Unfortunately, these studies are limited to the past few decades and thus are not long enough to determine natural background levels. Considering this limitation, ice core records offer the ideal natural archive for inferring the past atmospheric compositions of anthropogenic pollutants, as they can provide well-preserved, high-resolution, multi-parameter glaciochemical data that predate the instrumental era.

Ice core records have previously been utilized to reconstruct atmospheric heavy metal concentrations in the northern hemisphere (e.g. Boutron et al., 1991; Eichler et al., 2012, 2014; Hong et al., 2009; Kaspari et al., 2009; Li et al., 2006; McConnell et al., 2006; Osterberg et al., 2008; Schwikowski et al., 2004; Shotyk et al., 2005; Van de Velde et al., 2000). These records have captured and revealed the spatial and temporal variability in the rise of atmospheric heavy metal concentrations during the rapid industrialization of the twentieth century, as well as subsequent emission reductions, reflective of regional pollution abatement legislation (i.e. North America and Europe) (Boutron et al., 1991; Fischer et al., 1998; Preunkert et al., 2001; Schwikowski et al., 2004; Van de Velde et al., 2000), and/or declines in industrial production (e.g. Eastern Europe and Soviet Union) (Eichler et al., 2012, 2014).

By the end of the twentieth century, Asia was estimated to be the largest emitter of anthropogenic atmospheric pollutants, including trace elements (Pacyna and Pacyna, 2001). Central Asian countries (e.g. Kazakhstan, Kyrgyzstan, Uzbekistan), along with western China, contain large-scale mining industries and agricultural lands that have severely polluted the regional ecosystems, impacting human health (UNEP, 2003; WHO, 2001). High natural background levels of dust, originating from the arid regions of central Asia and western China (e.g. Kyzyl Kum, Kara Kum, Aral Sea region) and Taklimakan Desert), can conceal anthropogenic inputs and make the distinction between natural and anthropogenic sources more complex. Therefore, high-elevation Asian ice cores, further removed from dust influences, are essential to help determine the impact of atmospheric heavy metal pollutants and assess natural background concentrations.

Previous Asian trace element ice core records that span multiple decades suggest that onsets of discernable anthropogenic inputs vary. Pb, Cd and Cu begin between the 1930s and 1940s at Belukha (Eichler et al., 2012, 2014), Bi, U, Cs, As, Mo, Sn, and Sb from Everest (Himalayas) (Kang et al., 2007; Kaspari et al., 2009; Hong et al., 2009) and Sb, Bi, Pb from Muztagh Ata (eastern Pamir) begin increasing between the 1950s and 1970s (Y. Li et al., 2006). Minor contributions of Sb, Bi, and Pb have been suggested at Miaoergou glacier (eastern Tien Shan) between 1953 and 2004 (Liu et al., 2011).

In the central Tien Shan, previous studies on trace elements have been limited, with the longest available records representing only a few years (1992–1998) (Kreutz and Sholkovitz, 2000). Here we present the first high-resolution multi-decadal (1908–1995) trace element records from Inilchek glacier (42.26°N, 80.42°E, 5120 m a.s.l; Fig. 1a), located in the central Tien Shan, focusing on Pb, Cd and Cu concentrations. Inilchek Glacier serves as an excellent archive to reconstruct the regional evolution of anthropogenic pollutants, due to its proximity to major Soviet and Chinese (western province of Xinjiang) industrial and agricultural centers that developed rapidly during mid-late twentieth century.

2. Methodology

2.1. Ice core collection and chemical analysis

In the summer of 2000, a collaborative ice core drilling expedition from the Climate Change Institute (University of Maine), the University of Idaho and the University of New Hampshire was conducted on the Inilchek glacier (42.26°N, 80.42°E, 5120 m a.s.l), located in the Tien Shan in Kyrgyzstan. Two ice cores were retrieved during the expedition using the ECLIPSE solar powered electromechanical drill (Blake et al., 1998; Gerasimoiff and Wake, 2001) and were returned frozen to the U.S. for analysis (Kreutz et al., 2003). Borehole temperature profiles were constant and were recorded at −12 °C between 10 m and 50 m and −11.2 °C at 100 m and 160 m, and stratigraphy profiles revealed negligible snowmelt (Aizen et al., 2001). This paper presents the methodology and data from the higher elevation core, Core 2 (160.48 m, 5120 m a.s.l.).

Core 2 was processed using a discrete sampling (DS) method. Samples were sectioned on a modified band-saw set (stainless-steel blades; tabletops and saw guides covered with teflon) and were regularly cleaned with ethyl alcohol and deionized (DI) water (>18.2 MΩ). Sample resolutions between 8 and 160 m depth were 0.10 m. Each individual sample outer surface was scraped in a clean cold room using a clean plastic lathe with pre-cleaned ceramic blades wearing a non-particulating tyvek suit, face mask and wrist-length polypropylene (PP) gloves. Samples were then placed into Whirlpak bags and melted at room temperature. A total of 1510 co-registered samples were collected into high-density polyethylene (HDPE) vials and polypropylene (PP) vials for analysis of stable water isotopes ($\delta^{18}O$ and δD) and trace elements (e.g. Al, As, Ca, Cd, Co, Cr, Cu, Fe, Li, Mn, Na, Pb, S, Ti, V). Vial-cleaning procedures for elemental analysis followed Osterberg et al. (2006). Stable water isotopes were analyzed at the Climate Change Institute (CCI) and the University of Idaho using a Micromass Isoprime ion chromatograph, a VG/Micromass SIRA and Isoprime magnetic sector SIRA (Stable Isotope Ratio Analysis) mass spectrometer configured in continuous flow mode with an Eurovector Pyr-OH peripheral with LAS (Liquid Auto Sampler). Analysis of major and trace elements were conducted at CCI using a Thermo-Finnigan Element 2 inductively coupled plasma sector field mass spectrometer (ICP-SFMS), respectively. The ICP-SFMS is coupled with a microflow nebulizer/desolvation introduction system to reduce potential spectroscopic interferences (Field and Sherrell, 2003; Gabrielli et al., 2006). ICP-SFMS samples were acidified to 1% with double-distilled HNO_3 and spiked with 1 ppb of indium as an internal standard under a class 100 High Efficiency Particle Air (HEPA) clean bench, and allowed to react with the acid for ten days before being frozen. Samples were melted at room temperature approximately 24 h prior to analysis. A statistical summary of major and trace elements is presented in Table 1. In addition, Core 2 was analyzed at Lamont-Doherty Earth Observatory for ^{137}Cs at approximately 1 m sample resolution using outer ice core cuts.

2.2. Inilchek time-scale

The Inilchek (Core 2) was annually dated to 1908 AD at a depth of ~160 m. The depth-age scale was based primarily on the annual layer counting (ALC) of clear sub-annual (seasonal) variation of stable water isotopes ($\delta^{18}O$ and δD) (Fig. 2a.). Although the majority of precipitation in the Inilchek Valley occurs during the summer

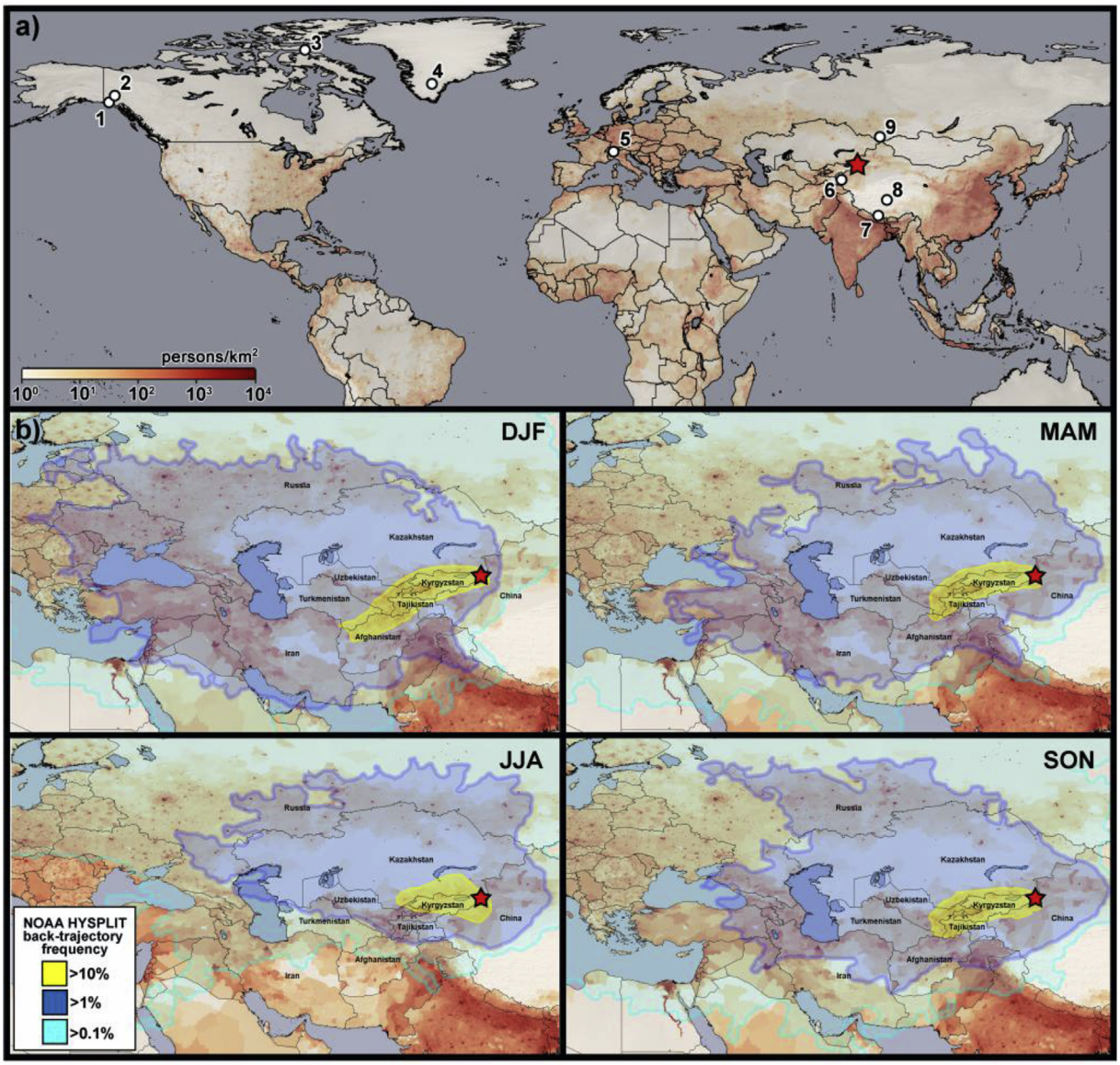

Fig. 1. a) Map showing the location of the Inilchek glacier (red star), Northern Hemisphere ice core sites discussed in the text (1- Logan, 2-Eclipse, 3-Devon Island, 4-ATC2, 5-Colle Gnifetti, 6-Muztagata, 7-Dasuopu, 8-Geladaindong, 9-Belukha. b) Seasonal NOAA HYSPLIT 7-day back trajectories frequency plots for the period 1950–1995 using NCEP reanalysis 1. Back trajectories were run every 12 h. Population density data from Center for International Earth Science Information Network–CIESIN (2005). (2-column image). (For interpretation of the references to colour in this figure legend, the reader is referred to the web version of this article.)

(Aizen et al., 1997; Kreutz and Sholkovitz, 2000), physical stratigraphy studies at Inilchek suggest that sufficient winter precipitation exists and that sine wavelike variability of δ ^{18}O and δD most likely includes January–December accumulation (Aizen et al., 2004; Kreutz and Sholkovitz, 2000). The variability of stable water isotopes (δ^{18}O and δD) is assumed to represent a first-order relationship with temperature and is based on Inilchek physical stratigraphy and regional precipitation studies that reveal strong correlations between temperature and δ ^{18}O ($r^2 = 0.82$) (Kreutz et al., 2003; Yao et al., 1999). Therefore, more depleted isotope values represent colder periods (e.g. mid-winter) and less depleted stable isotopes represent warmer periods (e.g. mid-summer). Secondary ALC parameters relied on seasonal deposition of elemental species (e.g. Ca, Pb). In addition to ALC, the depth-time scale was determined utilizing ^{137}Cs activity (Fig. 2a). ^{137}Cs activity rises above natural background levels between the mid-1950s and early 1960s reflecting the period of above ground nuclear testing. The maximum ^{137}Cs peak corresponded with ALC year 1963 reflecting the greatest amount of fallout from above ground nuclear weapons testing (UNSCEAR, 2000) prior to the adoption of a ban on atmospheric nuclear weapons testing. Dating uncertainties are estimated at ±0 years at 1963 (~78 m) and ±1 years at 1923 (~138 m) and ±3 at 1908 (159 m).

3. Results and discussion

3.1. Seasonal variability

Sub-annual time-series (~18 samples/year between 1908 and 1995) were compared to stable isotopic ratios (δ^{18}O and δD) to help identify seasonal timing. Element concentrations suggest primary deposition within the relatively warmer periods of the year (e.g. spring-autumn). However, Pb and Cd generally display concentration maxima during the warmest periods (e.g. summer) (Fig. 2b).

Table 1
A statistical summary of major and trace element concentrations determined at Inilchek.

Analyte	Mean	Median	SD[a]	min	max	WB blank[b]	WBDL[c]	IDL[d]	%WBDL[e]
Al (μg/L)	179	104	290	4	5641	0.05	0.14	0.04	0.08
As (ng/L)	248	164	377	7	8213	0.18	0.53	–	0.21
Ca (μg/L)	1708	1038	2899	52	60608	0.33	0.98	0.11	0.06
Cd (ng/L)	18	9	80	0	2905	0.03	0.08	0.03	0.48
Co (ng/L)	174	95	361	1	8545	0.05	0.16	0.41	0.09
Cr (ng/L)	356	188	688	3	12993	0.23	0.69	0.14	0.19
Cs (ng/L)	5.00	2.91	7.50	0.09	122	0.01	0.02	0.01	0.42
Cu (ng/L)	619	303	1344	5	24723	1.69	5.06	3.30	0.82
Fe (μg/L)	222	119	385	4	6854	0.02	0.07	0.01	0.03
Li (ng/L)	410	216	929	3	21640	3.11	9.34	0.04	2.28
Mn (ng/L)	8874	5910	12527	186	248953	0.58	1.73	1.00	0.02
Na (μg/L)	193	101	322	0.3	4764	1.31	3.92	–	2.03
Pb (ng/L)	654	376	950	11	14087	0.21	0.64	0.20	0.10
S (μg/L)	209	121	283	3	3869	0.33	0.98	0.29	0.47
Ti (ng/L)	5794	3271	9936	106	206240	1.54	4.61	0.70	0.08
V (ng/L)	360	213	570	6	11789	0.50	1.51	0.10	0.42

[a] SD = Standard Deviation of sample data.
[b] Median of 10 DI water samples collected from Whirlpak bags (WB).
[c] Whirlpak bags detection limits (WBDL) calculated by 3σ of 10 DI water samples from Whirlpak bags.
[d] Instrument detection limits (IDL) calculated by 3σ of 10 DI water samples for soluble ions and elements Osterberg et al. (2006).
[e] Whirlpak bags detection limit percentage of mean Inilchek glacier sample.

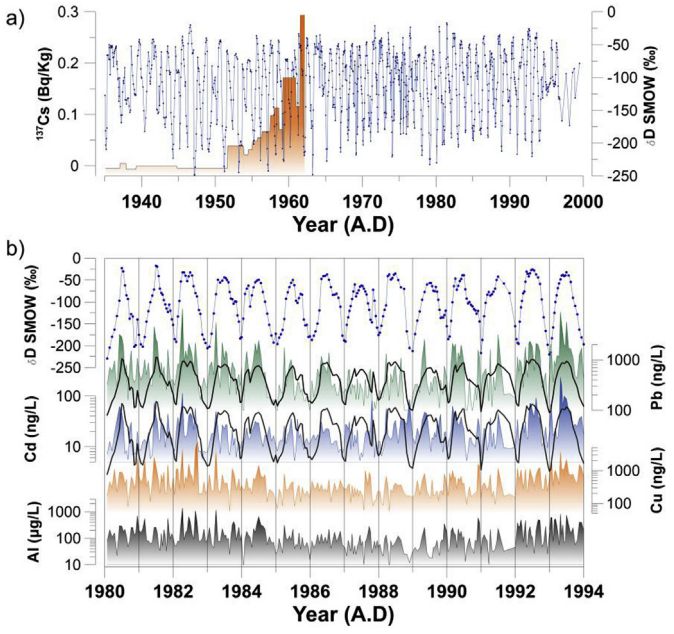

Fig. 2. Inilchek ice core timescale development: a) Seasonal δD variation and ^{137}Cs profile. b) Example of sub-annual variations of δD, Pb, Cd, Cu and Al. Black-lines representing δD profiles are overlain Pb and Cd to highlight seasonal timing. (1.5-column image).

Based on regional weather station data (e.g. Tien Shan (~3600 m) and Chonashu (~2,800 m)) ~50% of precipitation occurs between June and August (Central Asia Database), however at higher elevations up to 80% summer precipitation has been suggested (Aizen et al., 1997; Kreutz et al., 2001). Overall depositional timing of elements (spring-autumn) coincides with enhanced regional atmospheric entrainment of dust aerosols throughout central Asia (Indoitu et al., 2012). However, due to the high elevation of the Inilchek site, element timing may equally be a function of seasonal planetary boundary layer (PBL) processes that control the exchange of aerosols into the free troposphere. During warmer seasons (e.g. summer) vertical convective transport is enhanced to higher elevation regions, while it is impeded during colder seasons (e.g. winter) (Schwikowski et al., 2004; Eichler et al., 2014). Seasonal back-trajectory frequency analysis shows that Inilchek air-masses are primarily westerly and thus likely receive aerosols from central Asian countries (e.g. Kyrgyzstan, Kazakhstan, Tajikistan, Turkmenistan and Uzbekistan), Russia, western China, the Middle East and Europe (Fig. 1b). However, the highest percentage of back-trajectory frequencies (>10%) extended over Kyrgyzstan, southern regions of Kazakhstan, eastern Uzbekistan and western China. Winter (DJF), spring (MAM) and autumn (SON) reveal generally similar high frequency patterns, which suggest more westerly air masses. Summer (JJA) trajectories, however, although reflecting a westerly flow, suggest more trajectories originating from the north, south and east of Inilchek (Fig. 1b). This variance in trajectories is likely a result of summertime weakening of westerly circulation strength, which allows greater meriodional flow. At Inilchek, summertime southeasterly Föhn winds, that transport air masses from Xinjiang Province, China, were reported to occur 33% of the time (Aizen et al., 1997) and were cited to explain loess proxy variability of Chinese loess in a 1998 shallow ice core (Kreutz and Sholkovitz, 2000).

3.2. Empirical Orthogonal Function (EOF) analysis

Empirical Orthogonal Function (EOF) analysis was performed on sub-annual samples to reveal shared variance and help identify common sources and/or transport pathways between elements (Supplementary Table 1) (Meeker et al., 1995). EOF 1 represents ~64% of the total variance and is strongly loaded (>85%) by common dust tracers (e.g. Al and Ti) as well as significant loadings of potential anthropogenic species (e.g. Pb (48%) and Cu (59%)), suggesting a potentially combined natural and anthropogenic signal via common transport pathways. EOF 2 represents ~10% of the total variance and is primarily loaded by common evaporite (e.g. gypsum ($CaSO_4 \cdot 2H_2O$) and halite (NaCl)) derived dust species (Ca, S and Na) that are abundant throughout central Asia (International Center for Agricultural Research in the Dry Areas (ICARDA), 2008). Similarly, EOF 4, which is singularly and strongly loaded by Ca, likely represents calcareous ($CaCO_3$) soils that are abundant through central Asia. EOF 3, 5 and 6, which together represent ~14% of the total variation, are significantly loaded by Pb, Cd, and Cu and are

suggestive of anthropogenic sources, such as non-ferrous metal production, fertilizers and fossil fuel burning (e.g. coal and gasoline consumption) (Pacyna and Pacyna, 2001).

3.3. Twentieth century trends of Pb, Cd and Cu concentrations

Inilchek element time-series of Pb, Cd and Cu are presented in Fig. 3a. Annual concentrations are reported rather than flux, as dry vs. wet deposition rates are not well constrained and there are no correlation strengths between annual element concentrations and annual accumulation rates to justify flux corrections (Supplementary Table 2). Annual concentration time-series of Pb, Cd and Cu display decadal trends marked by short-term interannual variability. Multi-year trends in Pb and Cd reveal relatively low and stable concentrations during the 1908–1950 time-period followed by increases between the late 1950s and late-1970s (~factors of 5 and 4, respectively). Subsequently during the 1980s, Pb and Cd concentrations both decrease; however, Pb exhibits a much larger magnitude and longer duration change, reaching pre-1970 concentrations by the late 1980s. Cd concentrations begin to increase in the mid-1980s and exceed pre-1950 concentrations by a factor of ~6.5 during the early-mid 1990s. Similarly, Pb concentrations begin to rise in the late-1980s, to concentrations similar to the 1970s. Cu, relative to Pb and Cd, exhibits greater multi-year and inter-annual variability during the 1908–1950 time-period. Post-1960, Cu displays similar rises (although lesser magnitude, ~factor of 3) to the early 1980s, followed by declines during the 1980s and rises during the early-mid 1990s. Similar to Cd, multi-year Cu concentrations were highest in the 1990s. Based on the low concentrations during the early 1900s and the significant increases during the mid-late twentieth century, Pb, Cd and Cu records are suggestive of large-scale industrial and agricultural activities.

3.4. Natural vs. anthropogenic sources

Natural sources of Pb, Cd, and Cu include mineral dusts, sea salts, volcanic emissions, forest fires, and biogenic emissions (Nriagu, 1989). Due to the abundance of regional dust sources in central Asia, natural variations from atmospheric dust concentrations potentially reaching Inilchek cannot be excluded. To account for natural crustal inputs, excess (ex) and enrichment factor (EF) calculations were utilized to characterize the non-crustal contributions of the element time-series. Both calculations were used and examined to limit potential bias, including ubiquitous global upper continental crustal (UCC) element ratio assumptions and potential element dissolution rate variability during acid digestion that may impact EF values (Rhodes et al., 2011). Excess concentrations were derived using the equation: Excess [x] fraction = x − [*R*][r], where x = element of interest, r = conservative crustal element and R = reference ratio [x/r]. R represents an Inilchek ice core element ratio from the 1908–1920 reference baseline. The time-period 1908–1920 was selected as it is the oldest part of the ice core and pre-dates large scale Soviet industrialization in central Asia, which did not begin until the late 1920s (Roudik, 2007). EF values were calculated using the equation: $EF\ [x] = [x/r]_{sample}/[x/r]_{UCC}$, where x = the element of interest and r = the conservative crustal element. UCC concentrations were taken from Wedepohl (1995). Previous research suggests that EF values between +10 and −10 are indicative of dominant inputs from rock/soil dust, while EF values > 10 suggest non-crustal (e.g. anthropogenic) influences (Barbante et al., 2003). Commonly assumed dust tracers and EOF 1 dominate (>84%) elements Al, Ti, Mn and V, were selected as conservative crustal references. Multiple reference elements were selected to reduce any bias from a single element. Inilchek ex and EF time-series of Pb, Cd and Cu are presented in Fig. 3b.

Based on ex concentrations and EF value trends, discernable levels of anthropogenic Pb and Cd begin to reach Inilchek during the 1950s and 1960s. By the mid-late 1970s non-crustal inputs account for ~50% of the loading. Pb_{ex} and Pb_{EF} generally display decreases during the 1980s and increases into the 1990s, with ex concentrations representing ~40–50%. Cd_{ex} and Cd_{EF} display increases during the mid-1980s and 1990s represent between ~60 and 80%. In contrast, Cu_{ex} and Cu_{EF} suggest primarily crustal sources with discernable multi-year, non-crustal inputs (>0 for ex and

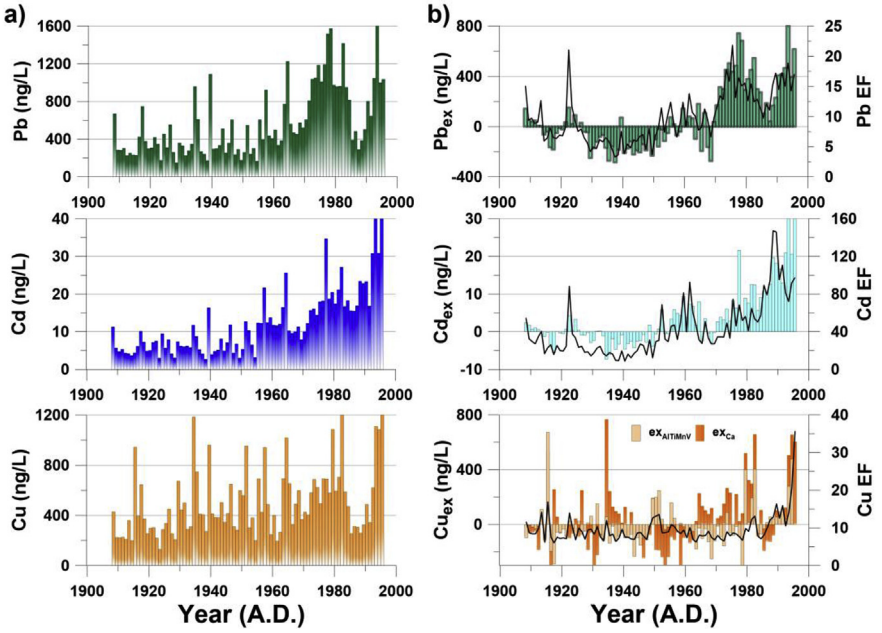

Fig. 3. a) Annual concentrations of Pb, Cd and Cu. b) Annual excess (ex) (bar) and enrichment factor (EF) (line) time-series of Pb, Cd and Cu time-series. For Cu_{ex} time-series, tan bars represent ex concentration using crustal reference elements Al, Ti, Mn and V; orange bars represent ex concentration using crustal reference element Ca. (2-column image)

>10 for EF) only beginning the late 1970s and reachingmaximums in the 1990s.

Here we investigate the potential spatial and temporal limitations of utilizing conservative crustal species assumptions. Inilchek glacier is in close proximity to central Asian industrial and agricultural regions, which were rapidly expanding during the mid-1900s. Soviet Union (SU) mineral mining increased rapidly between the 1950s-1970s, including mining of conspicuous sources of assumed conservative crustal species, such as Al (bauxite) and Ti which increased in production during this period by factors of 11 and 55, respectively (Rubinstein, 2002). Bauxite mining requires large-scale excavation of open pit mines that entrain dust during overburden removal and expose highly enriched Al and other heavy metal waste sources, such as tailings, to aeolian processes. The Torgay mine, located in Arkalyk, Kazakhstan, began operations in 1955 and became a major source of bauxite in the SU (Mining-Atlas, n.d.). Hence, the determination of non-crustal contributions, based on assumed conservative crustal species (e.g. Al, Ti, Mn, V), at Inilchek may be significantly underestimated due to its close proximity to large mining activities. Support for post-1950 anthropogenic Al was reported regionally in the Belukha ice core, and attributed to enhanced mining activities (Eichler et al., 2012, 2014).

At Inilchek, pre-1950s comparison of Pb and Al is prominently highlighted by distinct differences in baseline trends, suggesting varying sources (Fig. 4). Al concentrations display significant increases/decreases between 1930 and 1950, while Pb remains stable. In contrast, post-1950, Pb and Al display similar baseline trends as well as reaching time-series baseline concentration maximums, that coincide with intensified anthropogenic activities characteristic of the mid-late twentieth century, therefore potentially representing significant anthropogenic contributions, rather than only

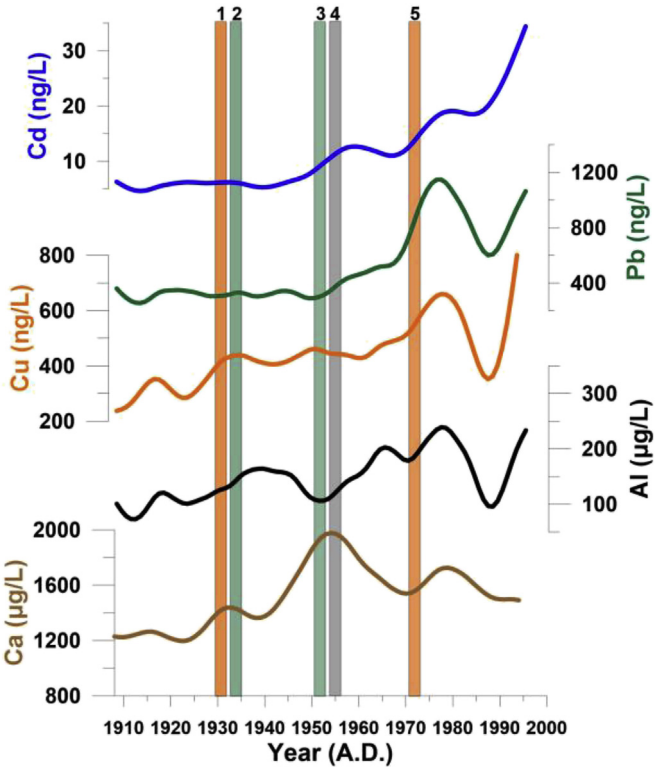

Fig. 4. Robust splines (tension 0.001) of annual Cd, Pb, Cu, Al and Ca time-series. Numbered bars represent initial operations at mineral mining/smelting complexes 1) Balkhash 2) Shymkent 3) Almalyk 4) Torgay 5) Zhezkazgan. (1-column image).

natural dust emissions. Global estimates of anthropogenically-entrained dust vary substantially ranging from minor contributions (Tegen et al., 2004; Mahowald and Luo, 2003) to upper limits of 50% (Luo et al., 2003). Additionally, regional dust storm activity may control Al element concentrations. Previous work by Indoitu et al. (2012) examined dust storm observations from central Asian meteorological stations for the period 1935 to 2005 and found that regionally, the 1940s to 1960s was the dustiest period, with regional decreases occurring during the 1980s and remaining low through the 1990s. An exception to regional trends was in the northern Aral Sea region (e.g. Aralsk), where dust storm activities were highest in the 1980s and 1990s. The increases in dust storms have been attributed to the desiccation of the Aral Sea (Indoitu et al., 2012), which began in the 1960s and by 1989 had lost ~40% of its area, exposing large areas of entrainable sediments (Micklin, 2007). Overall regional dust storm trends and northern Aral Sea trends do not coincide with Inilchek Al trends that display 1970s maximums, but rather regional dust storm trends coincide with Ca that exhibit the highest concentrations during the 1950s (Fig. 4). Similarly, dust storm activity to the south and east of Inilchek in Xinjiang has exhibited long-term declines since the 1950s and 1960s to the end of the 1990s (Qian et al., 2002; Wang et al., 2004).

Ex calculations of Pb, Cd and Cu, using only Ca as an assumed conservative crustal reference, reveal similar trends, however higher concentrations during the 1970s and 1990s and lower concentrations in the 1980s, potentially suggesting underestimations of ex concentrations using crustal reference elements Al, Ti, Mn and V. Cu_{ex} concentrations suggest multi-year, non-crustal contributions, beginning in the late 1960s and increasing through the early 1980s, representing 40–50% of the Cu load, that in the mid-late 1980s and 1990s increased 0 and ~40%, respectively. EF values also reveal similar trends, although overall, values are significantly lower, resulting from abundant calcareous soils in central Asia (ICARDA, 2008). Mean Inilchek Ca/Al ratios are ~30 times larger than UCC ratios. A previous shallow core from Inilchek that utilized HF-digested samples reported Ca/Al ratios to be 200 times the UCC ratio (Kreutz et al., 2003).

3.5. Anthropogenic sources and northern hemispheric trends of Pb, Cd and Cu

To help verify anthropogenic contributions to atmospheric chemistry, Inilchek time-series were compared to previously compiled historical records of mineral production and/or consumption (Historical Database of the Global Environment (HYDE) database; Food and Agriculture Organization (FAO) database; British Geological Survey (BGS) database; British Petroleum (BP) database). Inilchek Pb concentrations display similar trends to Soviet Union (SU)/Commonwealth of Independent States (CIS) Pb production and smelting (HYDE data), with corresponding maxima during the mid-late 1970s and rapid declines in the 1980s (Fig. 5a). We note the potential bias of comparing national level production with a specific site location, however, Kazakhstan, as of 1975, produced 73% of the SU/CIS Pb smelter output (Rubinstein, 2002; Jenson et al., 1983). Summertime (JJA) back-trajectories suggest primarily sources from the west in Krygzstan and south Kazakhstan, including the Fergana Valley and the cities of Shymkent Bishkek, Karokol, and Almaty (Fig. 6). Shymkent and the Fergana Valley are the most probable sources. The first Pb smelter was built in Shymkent during the 1930s and the city has subsequently represented, at times, 70–90% of SU Pb manufactured (USGS, 1994). The Fergana Valley has previously been identified as a major source of CIS Pb emissions (NILU, 1984). It contains several large Pb mines, including the Almalyk mining-metallurgical complex, which was built in the early 1950s, coinciding with the initial rise in Pb at

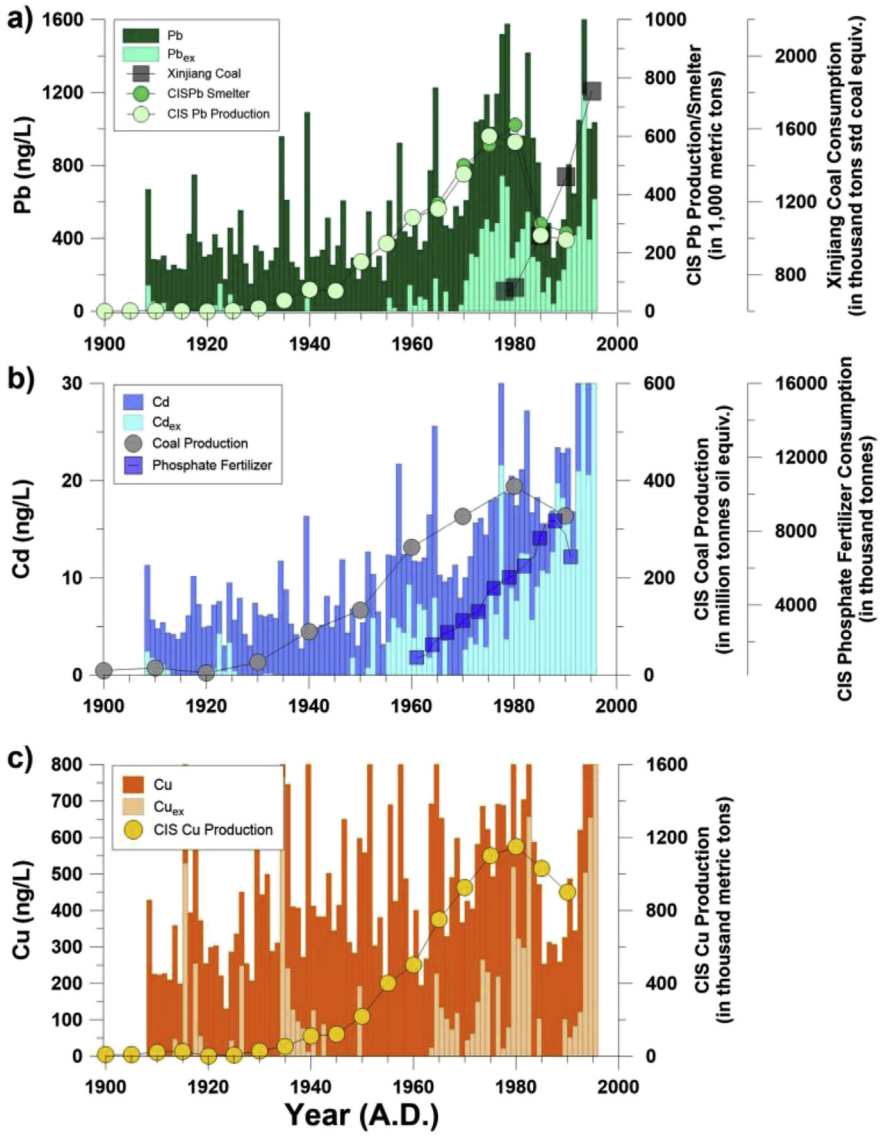

Fig. 5. Comparisons between Inilchek Pb, Cd and Cu and Production and Consumption data a) Inilchek Pb and Pb_{ex} compared CIS Pb production (light green circles), CIS Pb smelting (dark green circles) and Xinjiang coal consumption (black squares). b) Inilchek Cs and Cd_{ex} compared CIS Coal production (gray circles) and CIS phosphate fertilizer consumption (blue squares). c) Inilchek Cu and Cu_{ex} compared with CIS Cu production (yellow circles). (1.5-column image). (For interpretation of the references to color in this figure legend, the reader is referred to the web version of this article.)

Inilchek (Fig. 4). Kakareka et al. (2004) estimated that 1990 Pb emissions in the central Asian republics' (e.g. Kazakhstan, Kyrgyzstan, Uzbekistan) represented 60% industrial sources and 35% transportation sources, while stationary fuel combustion (e.g. oil and coal combustion) accounted for ~1%. Available SU light distillate data and direct gasoline consumption data suggest that Pb increased throughout the 1970s, reached a peak ~1980 and remained stable throughout the 1980s (BP data; Tretyakova and Kostinsky, 1987). Inilchek Pb records are consistent with a primarily Pb production signal, with considerable regional Pb emissions derived from the combustion of leaded gasoline, especially from densely populated areas, such as Almaty, Bishkek and the Fergana Valley. We are unaware of any Pb-additive reductions that took place in central Asia during the 1980s that can account for the Inilchek Pb record. A ban on Pb-additives in the region (e.g. Russia, Kyrgyzstan and Kazakhstan) was not implemented until the early 2000s.

In contrast to the 1950s to 1980s, Inilchek Pb concentration trends during the late-mid 1980s-1990s are not suggestive of CIS Pb production, which had been reduced following the collapse of the Soviet Union in 1991(BGS data). These Pb trends may reflect, in part, increases in urban traffic emissions in Kyrgyzstan and Kazakhstan, which were estimated at 24% between 1990 and 2000 (Balance and Pant, 2003), however, it may more likely reflect the rapid growth of pollutant sources from western China (i.e. Xinjiang Province) during the 1980s and 1990s. Between 1985 and 1995, Xinjiang energy production and consumption (primary coal and crude oil) increased by ~30% and ~50%, respectively (Tang et al., 2009) (Fig. 5a). Although NOAA back-trajectories exist year-round to justify pollutant inputs from nearby Xinjiang sources (e.g. Aksu located only ~100 km from Inilchek glacier), higher summertime concentrations of Pb coincide with seasonally weakened westerly transport and enhanced air mass transport from western China (Fig. 6). Comparisons between JJA back-trajectory frequencies suggest enhanced air mass transport from Xinjiang relative to the 1970s, and may additionally explain increased 1990s concentrations than

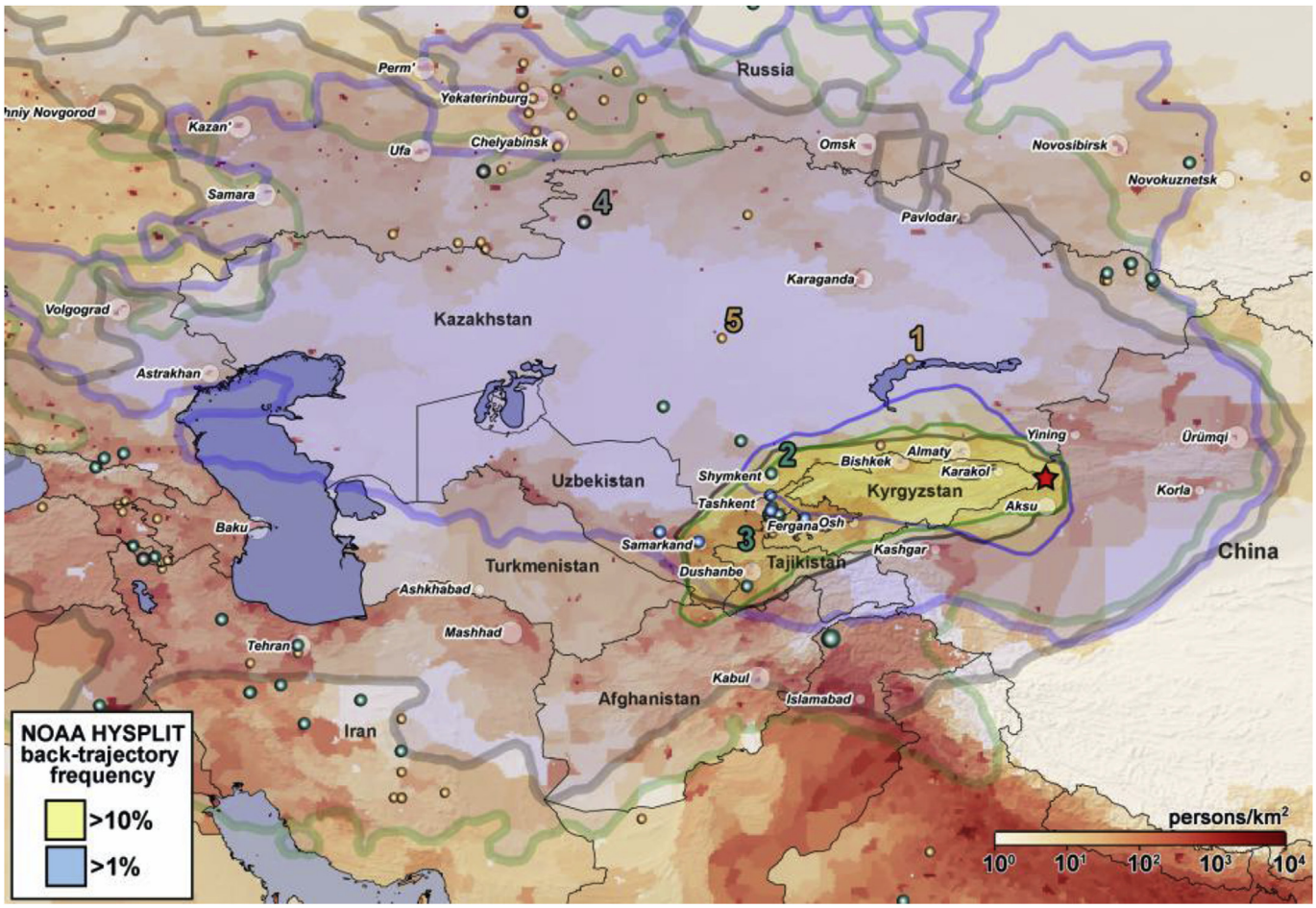

Fig. 6. Mineral and Fertilizer production locations denoted by colored circles (USGS database): Pb (green), Cu (orange), bauxite (gray) and fertilizers (dark blue). Inilchek glacier (red star). Numbered locations represent mineral complexes: 1) Balkhash 2) Shymkent 3) Almalyk 4) Torgay 5) Zhezkazgan. White circles indicate cities. Seasonal NOAA HYSPLIT 7-day back trajectories frequency plots for MAM (green borders), JJA (blue borders), and SON (dark-gray borders) during the period 1950–1995 using and NCEP reanalysis 1. Back trajectories were run every 12 h. Population density data from Center for International Earth Science Information Network–CIESIN (2005). (2-column image). (For interpretation of the references to color in this figure legend, the reader is referred to the web version of this article.)

only regional pollutant emission strength variability (CIS vs. Xinjiang) (Supplementary Fig. 1).

Anthropogenic sources of Cd in central Asia have primarily been suggested to originate from non-ferrous metal production (e.g. Pb and Cu) (Kakareka et al., 2004). CIS estimates of atmospheric Cd attribute ~70% to non-ferrous metal production and ~20% to fossil fuel combustion, although these estimates do not include phosphate fertilizers, a potential major source of Cd (Pacyna and Pacyna, 2001). Inilchek Cd displays similar trends to CIS Pb, Cu, and coal production (HYDE data) with decline onsets similar to Pb production and decline magnitudes similar to Cu production (Fig. 5b). In contrast, Cd_{ex} and Cd_{EF} trends suggest a stronger relationship to phosphate fertilizer consumption and production (FAO data), displaying similar increasing trends and simultaneous peaks in the mid-1980s, followed by declines to 1990. The non-ferrous metal and fertilizer industries, along with large agricultural areas in Fergana Valley, are the likely sources of Cd, as they are located within the highest air mass trajectory frequencies (Fig. 6). The Fergana Valley was identified as the largest emitter of SU Cd in 1979-80 (NILU, 1984). Additional Cd sources may include agricultural regions surrounding Bishkek and Almaty. The large increases in both Cd and Cd_{ex} during the 1990s cannot be explained by post-SU (1992–1995) Cd production and/or coal consumption data from central Asia which showed declines in the 1990s (BGS data; BP data). Rather, Cd inputs may reflect increases in Xinjiang fossil fuel burning and/or enhanced fertilizer (e.g. phosphate) use due to rapid increases in cotton production during the 1990s (Leiwen et al., 2005).

Inilchek Cu trends exhibit similar post-1950 trends with CIS Cu production (HYDE data), displaying increases until the late 1970s-early 1980s, followed by declines during the mid-late 1980s (Fig. 5c). Back-trajectories suggest sources may include major Cu smelting/refining complexes in Balkhash and Zhezkazgan (Kazakhstan), and Leninabad and Almalyk (Uzbekistan) (Fig. 6). Balkhash Cu is significantly sourced from the Kounrad mine, which started operations in the late 1920s and subsequently became one of the largest sources of Cu in the CIS (Rubenstein, 2002). Balkhash complex Cu production experienced a 25% decline in Cu production between 1979 and 1985 (International Monetary Fund, 1991). This decline is much larger than the complied CIS Cu production displays and reveals a greater similarity to Inilchek Cu declines during the same period. Extracting Cu commonly requires large open pit mines that emit dust during overburden removal, as well as exposing highly enriched mineral waste tailings to wind transport. *Fugitive dust*, containing high concentration heavy metal waste, enriched in elements such as Cu, Al, Fe, Mn, and As, may explain the common post-1950s trends exhibited by most Inilchek elements. High Cu and Cu_{ex} concentrations in the 1970s-early 1980s follow

the opening of the Zhezkazgan mining complex in Kazakhstan in the early 1970s (Fig. 4) (KAZ Minerals, 2015). The high Cu and Cu_{ex} concentrations exhibited during the 1990s do not reflect declining post-SU (1992–1995) Kazakhstan Cu production (BGS data). The extent and presence of non-ferrous metal production in Xinjiang prior to 1995 is unclear, however, other sources of Cu exist. Enhanced Inilchek Cu may reflect the increased use of Cu-fertilizers and/or Cu-herbicides/fungicides during the rapid expansion of agriculture in Xinjiang during the 1990s.

3.6. Northern hemispheric variability of Pb, Cd and Cu

Compilations of northern hemispheric ice core records are presented in Fig. 7 to illustrate regional onsets of anthropogenic contributions of Pb, Cd and Cu for the period of 1800–2000. Inilchek Pb (Fig. 7a) concentrations reveal similar trends to nearby sites Muztagata (East Pamir) and Belukha (Altai), displaying rapid increases between the 1950s-1970s and declines during the mid-late 1970s to 1980s. However, differences are apparent as Inilchek and Muztagata display increases between the late 1980s and mid-1990s, while Belukha shows declines into the 1990s. Muzagata and Inilchek sites are located in border regions between central Asian

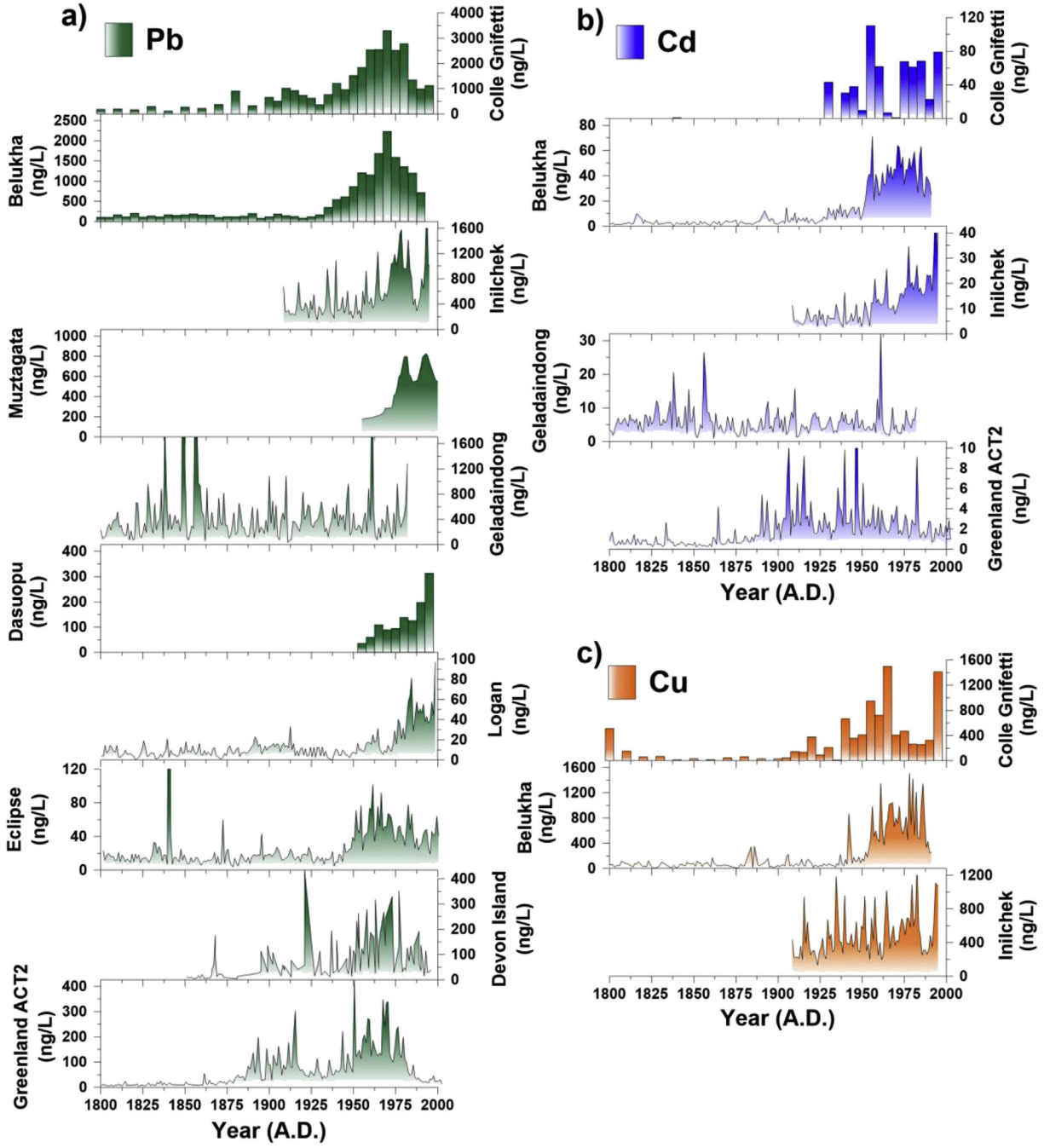

Fig. 7. Northern Hemisphere ice core records (references in text) a) Pb for data Colle Gnifetti, Belukha, Inilchek, Muztagata, Geladaindong, Dasuopu, Logan, Eclipse, Devon Island and Greenland ACT2. b) Cd data for Colle Gnifetti, Belukha, Inilchek, Geladaindong and Greenland ACT2. c) Cu data for Colle Gnifetti, Belukha, and Inilchek. (2-column image).

(e.g. Shymkent and Fergana Valley) and western Chinese (e.g. Kashgar and Aksu) industrial and agricultural regions. Therefore, these sites likely capture anthropogenic records containing both industrial SU Pb histories and the growth of energy consumption (e.g. coal and leaded-gasoline) in Xinjiang. Anthropogenic Pb at Belukha emerges 10–20 years prior to Inilchek, with maximum concentrations occurring slightly earlier between 1970 and 1975, followed by declines to the 1990s. These differences are likely a result of emission source regions. Belukha Pb trends (1935–1995) are attributed to Eastern European transportation and industrial sources (Eichler et al., 2012). Both records coincide with nationwide Soviet economic declines in the late 1970s and 1980s and therefore differences in timing may reflect varying regional-scale economics. In contrast to central Asian sites, western European (Colle Gnifetti) and North American (Greenland and Devon Island) sites, reflect earlier western industrialization, attributed to mid-to-late 19th century increases in industrialized coal burning and twentieth century increases in leaded gasoline usage. These records also display declines beginning in the early 1970s, although this has been attributed to strong air quality legislation and the phase-out of leaded gasoline, rather than economic factors (Schwikowski et al., 2004; McConnell et al., 2006; Shotyk et al., 2005).

East Asian and Indian anthropogenic Pb records have been derived from Logan and Dasuopu, respectively, revealing Pb increases beginning in the 1960s-1970s and persisting to the present (i.e. drill year) (Osterberg et al., 2008; Thompson et al., 2000; Huo et al., 1999). Despite the strong indications of significant anthropogenic Pb inputs on the periphery of the Tibetan Plateau (TP) (e.g. Dasuopu (Himalayas) and Muztagata (East Pamir)) by the 1960s (although these records offer a limited timeframe to access natural background concentrations as they date back only to ~1950), ice core records from Geladaindong (GL), in the interior of the Tibetan Plateau, suggest that anthropogenic Pb had not exceeded natural background dust concentrations by the late 1970s-early 1980s (Supplementary Table 3) (Grigholm et al., 2015). Interestingly, the Eclipse ice core, located near Logan in the Canadian Yukon, has been attributed to pollutants originating from both North America and eastern Asia. While Pb concentrations reveal similar declining trends to Greenland and Devon Island, $^{206}Pb/^{207}Pb$ ratios suggest increasing East Asian anthropogenic Pb sources (Gross et al., 2012).

The earliest anthropogenic Cd records (Fig. 7b) are from Greenland and display late ninetieth century rises and mid-twentieth century declines, attributed to North American and European coal consumption (McConnell and Edwards, 2008). While in Europe, Colle Gnifetti has been attributed to non-ferrous metal production displaying generally increasing concentrations to the late 1900s (Van de Velde et al., 2000). In central Asia, Belukha and Inilchek reveal abrupt increases in the early 1950s, reflecting rapid increases in non-ferrous metal production, as well as coal and fertilizer consumption. Belukha trends suggest that non-ferrous metal production and coal are major sources as concentrations decline post-1975. Inilchek may suggest stronger influences by phosphate fertilizer emissions pre-1990, while post-1990 sources are likely derived from enhanced fertilizer use and coal burning in Xinjiang. It is unclear whether Belukha experienced similar Cd rises during the 1990s, as available records begin in 1991. Cd records from Geladaindong suggest that by 1982 discernable Cd pollution was not reaching the interior of the Tibetan Plateau or that natural background concentrations of mineral dust were masking anthropogenic inputs (Supplementary Table 2) (Grigholm et al., 2015).

To our knowledge Cu records are only available from three sites in the northern hemisphere Colle Gnifetti (Van de Velde et al., 2000), Belukha (Eichler et al., 2014) and Inilchek (this work) (Fig. 7c). Colle Gnifetti suggests anthropogenic inputs (e.g. Cu production) in Europe, beginning in the early 1900s and displays increases until the ~1960s, followed by general declines to the 1990s and a large increase in the mid-1990s (Van de Velde et al., 2000). In central Asia, Belukha reveals a prominent shift post-1950, followed by increases to late 1970s – early 1980s, followed by declines to 1991, reflecting SU Cu production. However, baseline concentrations at Belukha suggest high concentrations during the mid-1960s, which is earlier than SU Cu production peaks and similar to Colle Gnifetti maximums. This may suggest that Belukha captured earlier European Cu emission peaks, as well as subsequent maximums of SU Cu. This interpretation is consistent with the long-distance westerly transport attributed to Belukha Pb from eastern Europe (Eichler et al., 2012). Interestingly, Belukha Cu concentrations reveal a greater frequency and magnitude of interannual variability post-1950, during dominant anthropogenic inputs, when compared to the pre-industrial era. This behavior may suggest more variable controls of Cu inputs from sources such as *fugitive dust* from open-pit mines and may suggest similar interannual variability controls of Inilchek Cu pre-1970, as open-pit mines such as Kounrad, have been in operation since the late 1920s. Coinciding high concentrations during the 1990s at Inilchek and Colle Gnifetti are likey unrelated due to source distance and varying long-term trends during the 1900s. Belukha Cu, post-1991, may exhibit similar trends to Inilchek during mid-1990s as it also receives air masses from western China provinces (e.g. Xinjiang).

4. Conclusions

This study presents the first high-resolution, multi-decadal (1908–1995) trace element ice core record from Inilchek glacier in the central Tien Shan. Seasonal variability of element concentrations and stable water isotope analysis reveal dominant warm period (e.g. summer) deposition. Decadal trends of trace element records reveal pronounced temporal baseline concentration maximums that are characteristic of post-1950 anthropogenic activities and indicate that atmospheric composition has been significantly altered at Inilchek during the twentieth century. Examination of Pb, Cd and Cu concentrations, along with non-crustal calculation estimates (i.e. excess and enrichment factor), reveal discernable anthropogenic inputs beginning in the 1950s and rapidly increasing to the late-1970s and early 1980s, by factors of up to 5, 6, and 3, respectively, relative to a 1910–1950 mean. However, due to the rapid growth of large-scale mining activities between the 1950s and 1970s, enhancing entrainment and enriching mineral dust compositions (e.g. Al, Ti, Mn, V, As), commonly assumed crustal reference species, may be biased and could underestimate non-crustal contributions at Inilchek. Therefore, complimentary methods (e.g isotopic analysis) should be used to differentiate element sources in future studies.

Between the 1950s and 1980s, Pb, Cd and Cu are highly reflective of CIS/FSU industrial and agricultural production trends, including non-ferrous metal, coal and fertilizer production and consumption. Complimentary JJA back-trajectory frequency analysis suggests pollutant sources originating primarily from southern Kazakhstan (e.g. Shymkent and Balkhash) and the Fergana Valley (located in Kazakhstan, Uzebekistan and Kyrgyzstan). Due to the decline of the Soviet economy in the 1980s and the subsequent collapse in the early 1990s, coupled with the rapid development of western China's industry and agriculture, dominate warm period (e.g. summer) pollutant air-mass transport concentrations have transitioned from central Asian sources to dominant emission sources in western China (e.g. Xinjiang Provence). Since 1995, central Asian countries (e.g. Kazakhstan, Uzbekistan and Kyrgyzstan) have re-established and, along with Xinjiang province, have expanded industrial activities (e.g. mining). Therefore, trace element records from Inilchek provide not only a historical record

of the rapid industrialization of central Asia during the twentieth century, but also provide a baseline for future monitoring of atmospheric composition in the region.

Acknowledgments

This research was supported by the NSF ATM 0754644 as part of the AICA (Asian Ice Core Array) project, NSF P2C2 AGS-1401899 Central Asian Climate Reconstruction, NSF Adaptation to Abrupt Climate Change IGERT program DGE-1144423, and Paleoclimate and Glaciological Reconstructions in Central Asia awards NSF AGS 0000561 and NSF AGS 0096323. We thank Timothy Kenna from the Lamont-Doherty Earth Observatory for ^{137}Cs analyses. The authors gratefully acknowledge the NOAA Air Resources Laboratory (ARL) for the provision of the HYSPLIT transport and dispersion model and/or READY website (http://www.ready.noaa.gov) used in this publication.

Appendix A. Supplementary data

Supplementary data related to this article can be found at http://dx.doi.org/10.1016/j.atmosenv.2016.01.030.

References

Aizen, V.B., Aizen, E.M., Dozier, J., Melack, J.M., Sexton, D.D., Nesterov, V.N., 1997. Glacial regime of the highest Tien Shan mountain, Pobeda-Khan Tengry massif. J. Glaciol. 43 (145), 503–512.

Aizen, V., Kreutz, K., Wake, C., 2001. Paleoclimate and Glaciological Reconstruction in Central Asia through the Collection and Analysis of Ice Cores and Instrumental Data from the Tien Shan FINAL REPORT. DOE Contract Number: FG07–00ID13906.

Aizen, V., Aizen, E., Melack, J., Kreutz, K., Cecil, L., 2004. Association between atmospheric circulation patterns and firn-ice core records from the Inilchek glacierized area, central Tien Shan, Asia. J. Geophys. Res. 109, 10.1029.

Balance, R., Pant, B.D., 2003. Environment Statistics in Central Asia: Progress and Prospects (ERD Work. ERD Work, Pap. Ser).

Barbante, C., Boutron, C.F., Morel, C., Ferrari, C., Jaffrezo, J.L., Cozzi, G., Gaspari, V., Cescon, P., 2003. Seasonal variations of heavy metals in central Greenland snow deposited from 1991 to 1995. J. Environ. Monit 5, 328–335.

Blake, E., Wake, C.P., Gerasimoff, M., 1998. The ECLIPSE drill: a field-portable intermediate depth ice coring drill. J. Glaciol. 175–178.

Boutron, C.F., Görlach, U., Candelone, J.-P., Bolshov, M.A., Delmas, R.J., 1991. Decrease in anthropogenic lead, cadmium and zinc in Greenland snows since the late 1960s. Nature. http://dx.doi.org/10.1038/353153a.

British Geological Survey. World Mineral Statistics and World Mineral Production Series. https://www.bgs.ac.uk/mineralsuk/statistics/worldArchive.html [January 17, 2015].

British Petroleum (BP) database. BP Statistical Review of World Energy. http://www.bp.com/en/global/corporate/energy-economics/statistical-review-of- world-energy.html [January 20, 2015].

Center for International Earth Science Information Network – CIESIN – Columbia University, United Nations Food and Agriculture Programme – FAO, and Centro Internacional de Agricultura Tropical – CIAT. 2005. Gridded Population of the World, Version 3 (GPWv3): Population Count Grid. Palisades, NY: NASA Socioeconomic Data and Applications Center (SEDAC). http://dx.doi.org/10.7927/H4639MPP. (accessed 13.02.15).

Eichler, A., Tobler, L., Eyrikh, S., Gramlich, G., Malygina, N., Papina, T., Schwikowski, M., 2012. Three centuries of Eastern European and Altai lead emissions recorded in a Belukha ice core. Environ. Sci. Technol. 46 (8), 4323–4330. http://dx.doi.org/10.1021/es2039954.

Eichler, A., Tobler, L., Eyrikh, S., Malygina, N., Papina, T., Schwikowski, M., 2014. Ice-core based assessment of historical anthropogenic heavy metal (Cd, Cu, Sb, Zn) emissions in the soviet union. Environ. Sci. Technol. 48 (5), 2635–2642. http://dx.doi.org/10.1021/es404861n.

Field, M.P., Sherrell, R.M., 2003. Direct determination of ultratracelevels of metals in fresh water using desolvating micronebulization and HR-ICP-MS: application to Lake Superior waters. J. Anal. At. Spectrom. 18 (3), 254–259.

Fischer, H., Wagenbach, D., Kipfstuhl, J., 1998. Sulfate and nitrate firn concentrations on the Greenland ice sheet 2. Temporal anthropogenic deposition changes. J. Geophys. Res. Atmos 103 (D17). http://dx.doi.org/10.1029/98JD01886.

Food and Agriculture Organization [Fertilizer Archive] [http://faostat3.fao.org/download/R/RA/E] [March 4, 2015].

Gabrielli, P., Barbante, C., Turetta, C., Marteel, A., Boutron, C., Cozzi, G., Cairns, W., Ferrari, C./, Cescon, P., 2006. Direct Determination of Rare Earth Elements at the Subpicogram per Gram Level in Antarctic Ice by ICP-SFMS Using a Desolvation System. Anal. Chem. 78 (6), 1883–1889. http://dx.doi.org/10.1021/ac0518957.

Gerasimoff, M., Wake, C.P., 2001. A reason for Resin. J. Glaciol. 47, 153.

Grigholm, B., Mayewski, P.A., Kang, S., Zhang, Y., Morgenstern, U., Schwikowski, M., , et al.Sneed, S., 2015. Twentieth century dust lows and the weakening of the westerly winds over the Tibetan Plateau. Geophys. Res. Lett. 42 (7), 2434–2441. http://dx.doi.org/10.1002/2015GL063217.

Gross, B.H., Kreutz, K.J., Osterberg, E.C., McConnell, J.R., Handley, M., Wake, C.P., Yalcin, K., 2012. Constraining recent lead pollution sources in the North Pacificusing ice core stable lead isotopes. J. Geophys. Res 117. D16307.

History Database of the Global Environment (2015). Retrieved March 23, 2015, from http://themasites.pbl.nl/tridion/en/themasites/hyde/productiondata/index-2.html.

Hong, S., Lee, K., Hou, S., Hur, S. Do, Ren, J., Burn, L.J., , et al.Boutron, C.F., 2009. An 800-year record of atmospheric As, Mo, Sn, and Sb in central Asia in high-altitude ice cores from Mt. Qomolangma (Everest). Himalayas. Environ. Sci. Technol. 43 (21), 8060–8065. http://dx.doi.org/10.1021/es901685u.

Huo, W., Yao, T., Li, Y., 1999. Increasing atmospheric pollution revealed by Pb record of a 7 000-m ice core. Chin. Sci. Bull. 44 (14), 1309–1312. http://dx.doi.org/10.1007/BF02885851.

International Center for Agricultural Research in the Dry Areas (ICARDA), 2008. Climatic and Soil Datasets for the ICARDA Wheat Genetic Resource Collections of the Eurasia Region. Retrieved from. http://geonet.icarda.cgiar.org/geonetwork/data/regional/GRU_NetBlotch/Doc/Report_NetBlotch.pdf.

Indoitu, R., Orlovsky, L., Orlovsky, N., 2012. Dust storms in Central Asia: spatial and temporal variations. J. Arid Environ. 85, 62–70. http://dx.doi.org/10.1016/j.jaridenv.2012.03.018.

International Monetary Fund, 1991. A Study of the Soviet Economy, vol. 3. OECD, London.

Järup, L., 2003. Hazards of heavy metal contamination. Br. Med. Bull. 68, 167–182.

Jensen, R.G., Shabad, T., Wright, A.W., 1983. Soviet Natural Resources in the World Economy. University of Chicago Press.

Kakareka, S., Gromov, S., Pacyna, J., Kukharchyk, T., 2004. Estimation of heavy metal emission fluxes on the territory of the NIS. Atmos. Environ 38 (40), 7101.

Kang, S., Zhang, Q., Kaspari, S., Qin, D., Cong, Z., Ren, J., Mayewski, P.A., 2007. Spatial and seasonal variations of elemental composition in Mt. Everest (Qomolangma) snow/firn. Atmos. Environ. 41 (34), 7208–7218.

Kaspari, S., Mayewski, P., Handley, M., Osterberg, E., Kang, S., Sneed, S., , et al.Qin, D., 2009. Recent increases in atmospheric concentrations of Bi, U, Cs, S and Ca from a 350-year mount Everest ice core record. J. Geophys. Res. 114 (D4), D04302.

KAZ Minerals, 2015. History (accessed June 20, 2015). http://www.kazminerals.com/en/about_us/history.

Knutson, E.O., Tu, K.W., 1996. Size distribution of radon progeny aerosol in the working area of a dry former uranium mine. Environ. Int. 22 (Suppl. 1), 617–632. http://dx.doi.org/10.1016/S0160-4120(96)00164-X.

Kreutz, K., Sholkovitz, E., 2000. Major element, rare earth element, and sulfur isotopic composition of a high-elevation firn core: sources and transport of mineral dust in Central Asia. Geochem. Geophys. Geosyst. 1.

Kreutz, K.J., Aizen, V.B., Cecil, L.D., Wake, C.P., 2001. Oxygen isotopic and soluble ionic composition of a shallow firn core, Inilchek glacier, central Tien Shan. J. Glaciol 47 (159), 548–554. http://dx.doi.org/10.3189/172756501781831819.

Kreutz, K., Wake, C., Aizen, V., Cecil, L., Synal, H., 2003. Seasonal deuterium excess in a Tien Shan ice core: Influence of moisture transport and recycling in Central Asia. Geophys. Res. Lett. 30 (18), 1922.

Leiwen, J., Yufen, T., Zhijie, Z., Tianhong, L., Jianhua, L., 2005. Water resources, land exploration and population dynamics in arid areas - the Case of the Tarim river Basin in xinjiang of China. Popul. Environ. 26 (6), 471–503. http://dx.doi.org/10.1007/s11111-005-0008-8.

Li, Y., Yao, T., Wang, N., Li, Z., Tian, L., Xu, B., Wu, G., 2006. Recent changes of atmospheric heavy metals in a high-elevation ice core from Muztagh Ata, east Pamirs: initial results. Ann. Glaciol. 43 (1), 154–159.

Liu, Y., Hou, S., Hong, S., Hur, S. Do, Lee, K., Wang, Y., 2011. High-resolution trace element records of an ice core from the eastern Tien Shan, central Asia, since 1953 AD. J. Geophys. Res. 116 (D12) http://dx.doi.org/10.1029/2010JD015191.

Luo, C., Mahowald, N.M., del Corral, J., 2003. Sensitivity study of meteorological parameters on mineral aerosol mobilization, transport, and distribution. J. Geophys. Res. 108, 4447,. http://dx.doi.org/10.1029/2003JD003483.

Mahowald, N.M., Luo, C., 2003. A less dusty future? Geophys. Res. Lett. 30, 1903,. http://dx.doi.org/10.1029/2003GL017880.

McConnell, J.R., Edwards, R., 2008. Coal burning leaves toxic heavy metal legacy in the Arctic. Proc. Natl. Acad. Sci. U. S. A. 105 (34), 12140–12144. http://dx.doi.org/10.1073/pnas.0803564105.

McConnell, J.R., Kipfstuhl, S., Fischer, H., 2006. The NGT and PARCA shallow ice core arrays in Greenland: a brief overview. PAGES Newsl. 14, 13–14.

Meeker, L.D., Mayewski, P.A., Bloomfield, P., 1995. A new approach to glaciochemical time series analysis. In: Delmas, R.J. (Ed.), Ice Core Studies of Biogeochemical Cycles, NATO ASI Series, vol. 130. Springer, Berlin, pp. 383–400.

Micklin, P., 2007. The Aral Sea Disaster. Annual Review of Earth and Planetary Sciences. http://dx.doi.org/10.1146/annurev.earth.35.031306.140120.

Mining Atlas (n.d.) Mining Atlas Online Portal. (assessed July 15, 2015) https://mining-atlas.com/operation/Torgay_Bauxite_Mine.php.

Nriagu, J.O., 1989. A global assessment of natural sources of atmospheric trace metals. Nature 338 (6210), 47–49. Retrieved from. http://dx.doi.org/10.1038/338047a0.

NILU, 1984. Emission Sources in the Soviet Union; Norwegian Institute for Air Research: Lillestrøm, Norway. NILU Report, 4/84.

Nriagu, J.O., Pacyna, J.M., 1988. Quantitative assessment of worldwide

contamination of air, water and soils by trace metals. Nature 333 (6169), 134–139. http://dx.doi.org/10.1038/333134a0.
Osterberg, E.C., Handley, M.J., Sneed, S.B., Mayewski, P.A., Kreutz, K.J., 2006. Continuous ice core melter system with discrete sampling for major ion, trace element, and stable isotope analyses. Environ. Sci. Technol. 40 (10), 3355–3361. http://dx.doi.org/10.1021/es052536w.
Osterberg, E., Mayewski, P., Kreutz, K., Fisher, D., Handley, M., Sneed, S., , et al.Bourgeois, J., 2008. Ice core record of rising lead pollution in the North Pacific atmosphere. Geophys. Res. Lett. 35 (5), L05810. http://dx.doi.org/10.1029/2007GL032680.
Pacyna, J.M., Pacyna, E.G., 2001. An assessment of global and regional emissions of trace metals to the atmosphere from anthropogenic sources worldwide. Environ. Rev. http://dx.doi.org/10.1139/er-9-4-269.
Preunkert, S., Legrand, M., Wagenbach, D., 2001. Sulfate trends in a Col du Dôme (French Alps) ice core: A record of anthropogenic sulfate levels in the European midtroposphere over the twentieth century. J. Geophys. Res. http://dx.doi.org/10.1029/2001JD000792.
Qian, W., L. Quan, and Shi, S. Variations of the dust storm in China and its climatic control, J. Clim., 15(10), 2002, 1216–1229, doi:10.1175/1520-0442(2002)0152.0.CO;2.
Rhodes, R.H., Baker, J.A., Millet, M.-A., Bertler, N.A.N., 2011. Experimental investigation of the effects of mineral dust on the reproducibility and accuracy of ice core trace element analyses. Chem. Geol. 286 (3), 207–221. http://dx.doi.org/10.1016/j.chemgeo.2011.05.006.
Roudik, P., 2007. The History of the Central Asian Republics. Greenwood Publishing Group.
Rubinstein, J., 2002. Non-ferrous Metal Ores: Deposits, Minerals and Plants. CRC Press.
Schwikowski, M., Barbante, C., Doering, T., Gaeggeler, H.W., Boutron, C., Schotterer, U., , et al.Cescon, P., 2004. Post-17th-century changes of European lead emissions recorded in high-altitude alpine snow and ice. Environ. Sci. Technol. 38 (4), 957–964. http://dx.doi.org/10.1021/Es034715o.
Shotyk, W., Zheng, J., Krachler, M., Zdanowicz, C., Koerner, R., Fisher, D., 2005. Predominance of industrial Pb in recent snow (1994–2004) and ice (1842–1996) from Devon Island, Arctic Canada. Geophys. Res. Lett. 32 (21), L21814. http://dx.doi.org/10.1029/2005GL023860.
Tang, L., University of Gävle, Department of Technology, U., Environment, B., 2009. Mapping the Energy Use in Xinjiang, Province of China. University of Gävle. Department of Technology and Built Environment.
Tegen, I., Werner, M., Harrison, S.P., Kohfeld, K.E., 2004. Relative importance of climate and land use in determining present and future global soil dust emission. Geophys. Res. Lett. 31, L05105. http://dx.doi.org/10.1029/2003GL019216.
Thompson, L., Yao, T., Mosley-Thompson, E., Davis, M., Henderson, K., Lin, P., 2000. A high-resolution millennial record of the South Asian monsoon from Himalayan ice cores. Science 289 (5486), 1916. Retrieved from file:///Users/bg/Documents/Papers/Science 2000 Thompson.pdf.
Tretyakova, A., Kostinsky, B.L., 1987. USSR, Motor Fuel Use and Conservation in Transportation and Agriculture, 1970 to 1984, vol. 3. Soviet Branch, Center for International Research, Bureau of the Census (U.S. Department of Commerce).
UNEP, 2003. Environment and Security. Transforming Risks into Cooperation. United Nations Enviromental Programme, Chatelaine.
UNSCEAR United Nations Scientific Committee on the Effects of Atomic Radiation, 2000. Sources and Effects of Ionizing Radiation. Report to the General Assembly. United Nations, New York.
USGS (United States Geological Survey), 1994. The Mineral Industry of Kazakhstan. http://minerals.usgs.gov/minerals/pubs/country/1994/9422094.pdf.
USGS (United States Geological Survey), Mineral Information: Europe and Central Eurasia. Retrieved March 20, 2015, from http://minerals.usgs.gov/minerals/pubs/country/europe.html.
Van de Velde, K., Boutron, C.F., Ferrari, C.P., Moreau, A., Delmas, R.J., Barbante, C., , et al.Cescon, P., 2000. A two hundred years record of atmospheric cadmium, copper and zinc concentrations in high altitude snow and ice from the French-Italian Alps. Geophys. Res. Lett. http://dx.doi.org/10.1029/1999GL010786.
Wang, X., Dong, Z., Zhang, J., Liu, L., 2004. Modern dust storms in China: an overview. J. Arid Environ. 58 (4), 559–574. http://dx.doi.org/10.1016/j.jaridenv.2003.11.009.
Wedepohl, K.H., 1995. The composition of the continental crust. Geochim. Cosmochim. Acta 59, 1217–1239. http://dx.doi.org/10.1016/0016-7037(95)00038-2.
World Health Organization, 2001. Environment and People's Health of China. United Nation Development Programme.
Yao, T., Masson, V., Jouzel, J., Stievenard, M., Weizen, S., Keqin, J., 1999. Relationships between d18O in precipitation and surface air temperature in the Urumqi River Basin, east Tienshan Mountains, China. Geophys. Res. Lett. 26 (23), 3473–3476.